

Collapse of a Bose Condensate with Attractive Interactions

José A. Freire¹ and Daniel P. Arovas²

¹*Centro Brasileiro de Pesquisas Físicas, Rua Dr. Xavier Sigaud 150, Rio de Janeiro-RJ, 22290-180 BRAZIL*

²*Department of Physics, University of California at San Diego, La Jolla, CA 92093, USA*

(June 10, 2021)

We examine the Gross-Pitaevskii (GP) model for Bose-Einstein condensates in parabolic traps with attractive interactions. The decay of metastable condensates is investigated by applying the instanton formalism to the GP field theory. Employing various dynamical trial states, we derive within a coherent state path integral approach a collective coordinate description in terms of the condensate radius, in agreement with (and extending) earlier results. We then solve numerically for the complete instanton field configuration and compare with the collective coordinate approach. Adjusting only the effective mass of the collective coordinate, the two schemes are then in good agreement.

PACS numbers:

I. INTRODUCTION

It is well known that a Bose gas with purely attractive interactions is unstable and will collapse to a state with no thermodynamic limit. However, in the presence of a harmonic confining potential, Ruprecht *et al.* [1] have shown that a *metastable* condensate exists, provided the particle number N is sufficiently small. The condition for a metastable condensate is $N < N_c$, with $N_c \propto \ell/|a|$, where ℓ is the quantum confinement length associated with the trap, and a is the s -wave scattering length; $a < 0$ corresponds to an attractive s -wave pseudopotential. Such is the situation with ${}^7\text{Li}$, for which $a = -(14.5 \pm 0.4) a_B$, where a_B is the Bohr radius [2]. Indeed, experiments by Bradley *et al.* [4] demonstrated the existence of metastable ${}^7\text{Li}$ condensates of limited particle number ($N < N_c$). Experiment and theory are in rough agreement on the value of N_c .

The metastable condensate has a finite lifetime – it tunnels quantum mechanically to an unstable higher density state, which then collapses. The tunneling process was described by Stoof [5] in terms of a collective coordinate $q(t)$ which parameterizes a Gaussian condensate density,

$$\rho(\mathbf{r}; q(t)) = N \left(\frac{1}{\pi q^2(t)} \right)^{3/2} \exp \left(-\frac{\mathbf{r}^2}{q^2(t)} \right). \quad (1)$$

The quantum mechanics of this collective coordinate arises from the more microscopic Gross-Pitaevskii (GP) field theory [6], which is itself a simplification inasmuch as interatomic potentials are therein replaced by an effective s -wave pseudopotential $g \delta(\mathbf{r})$. To compute the tunneling rate, one must examine the Euclidean action S_E for the GP model,

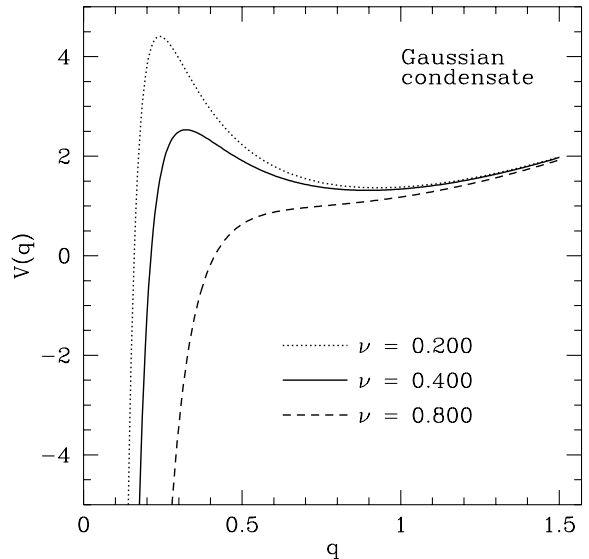


FIG. 1. The potential energy $V(q)$ derived from the Gaussian condensate profile of equation 1 for three values of ν . When $\nu < \nu_c = 16/15^{5/4} \simeq 0.542$ a metastable condensate exists.

$$S_E/\hbar = \int_{-\frac{1}{2}\beta}^{\frac{1}{2}\beta} d\tau \int d^3r \left\{ \bar{\psi} \partial_\tau \psi + \frac{1}{2} \vec{\nabla} \bar{\psi} \cdot \vec{\nabla} \psi + \frac{1}{2} r^2 \bar{\psi} \psi + \frac{1}{2} g (\bar{\psi} \psi)^2 \right\}, \quad (2)$$

Here and below distance is measured in units of $\ell = \sqrt{\hbar/m\omega}$, where m is the boson mass and ω is the trap frequency, time in units of ω^{-1} , and the fields ψ and $\bar{\psi}$ in units of $\ell^{-3/2}$. The coupling constant is then $g = 4\pi a/\ell$, where a is the (negative) s -wave scattering length. Periodic boundary conditions are enforced over the imaginary time domain $\tau \in [-\frac{1}{2}\beta, \frac{1}{2}\beta]$ where β is the inverse

temperature (units of $\hbar\omega$). Writing the complex order parameter field $\psi = \sqrt{\rho} \exp(i\theta)$ in terms of its amplitude and phase, Stoof formally integrates out the phase field $\theta(\mathbf{r}, \tau)$, resulting in an effective action $S_E[\rho(\mathbf{r}, \tau)]$ in terms of the density alone. Using the trial density from equation 1, the action functional becomes

$$S_E/\hbar = N \int d\tau \left\{ \frac{1}{2} m^* \dot{q}^2 + V(q) \right\}, \quad (3)$$

where m^* is an effective mass and

$$V(q) = \frac{3}{4} \frac{1}{q^2} + \frac{3}{4} q^2 - \frac{\nu}{\sqrt{2\pi}} \frac{1}{q^3} \quad (4)$$

and $\nu = N|a|/\ell = N|g|/4\pi$. A large value of N justifies the semiclassical treatment of this problem. The above effective potential $V(q)$ reflects the kinetic energy of confinement, the trap potential, and the attractive interparticle potential, respectively. Provided $\nu < \nu_c = 16/15^{5/4}$, $V(q)$ has a local minimum at $q = q_0$, corresponding to a metastable condensate. This state is isoenergetic with a denser condensate at $q = q_n < q_0$, and by considering motion in the inverted potential $-V(q)$ one constructs the usual bounce trajectory $q_b(\tau)$ [7] and from it the tunneling rate $\Gamma \propto \exp(-\Delta S_E/\hbar)$, where

$$\begin{aligned} \Delta S_E &= S_E[q_b(\tau)] - S_E[q_0] \\ &= N\hbar\sqrt{8m^*} \int_{q_n}^{q_0} dq \sqrt{V(q) - V(q_0)}. \end{aligned} \quad (5)$$

In this paper we shall use the formalism of coherent state path integration [8] to treat the problem of the collapsing metastable condensate. The instanton configuration for the GP field theory of equation 2 is described by two complex *fields* $\psi(\mathbf{r}, \tau)$ and $\bar{\psi}$. Restricting our attention to trial field configurations, we recover the collective coordinate effective action of equation 3.

II. DYNAMICS AND QUANTUM TUNNELING: COLLECTIVE COORDINATE APPROACH

Our goal is to numerically solve for the instanton of the GP action in the zero temperature limit by numerically solving for the saddle point of the action-extremizing equations. First, though, we concern ourselves with trial functions $\psi(\mathbf{r}, \tau)$ which yield a one-parameter effective action in the form of equation 3. In the zero temperature ($\beta \rightarrow \infty$) limit, the initial and final configurations, $\psi(\pm\frac{1}{2}\beta, \mathbf{r})$ should represent a metastable condensate. At the temporal midpoint $\tau = 0$, $\psi(0, \mathbf{r})$ represents the state of the field after it emerges from the tunnel barrier, *i.e.* a denser condensate whose real time evolution (according to the nonlinear Schrödinger equation) is unstable

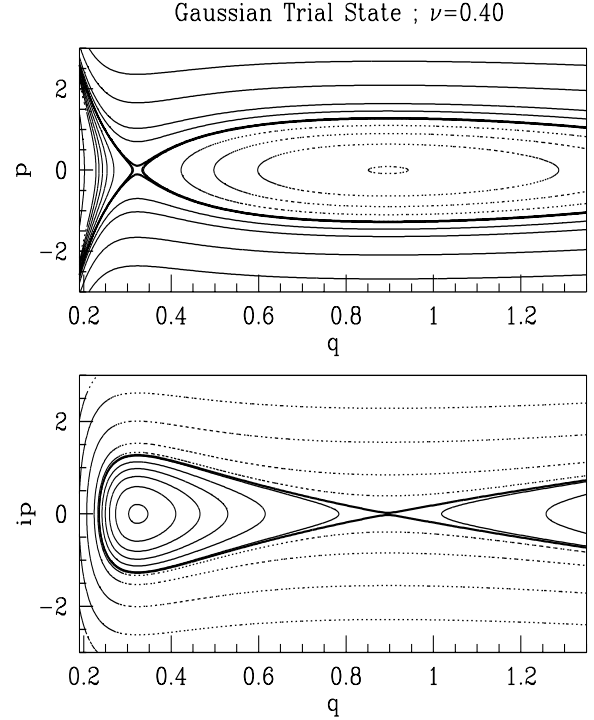


FIG. 2. Contour plots of $H(p, q)$ (top) and $H(ip, q)$ (bottom) for the Gaussian trial states ($\nu = 0.40$). Solid lines represent highs and dotted lines lows. (In the top graph, the low contours increase linearly while the high ones increase quadratically. In the bottom graph, the situation is reversed.)

towards collapse. To interpolate between these states, let us make the dynamical *Ansatz*

$$\psi(\mathbf{r}, \tau) = A \exp(-\alpha r^2) \quad (6)$$

$$\bar{\psi} = \bar{A} \exp(-\bar{\alpha} r^2). \quad (7)$$

where A , \bar{A} , α , and $\bar{\alpha}$ are functions of the time. Number conservation relates these quantities, since

$$N = \int d^3r \bar{\psi} \psi = \frac{\pi^{3/2} A \bar{A}}{(\alpha + \bar{\alpha})^{3/2}}. \quad (8)$$

Inserting our *Ansatz* into equation 2, we find

$$\begin{aligned} S_E/\hbar &= N \int d\tau \left\{ -\frac{3}{2} \frac{\dot{\alpha}}{\alpha + \bar{\alpha}} + 3 \frac{\alpha \bar{\alpha}}{\alpha + \bar{\alpha}} \right. \\ &\quad \left. + \frac{3}{4} \frac{1}{\alpha + \bar{\alpha}} - \frac{\nu}{\sqrt{2\pi}} (\alpha + \bar{\alpha})^{3/2} \right\}, \end{aligned} \quad (9)$$

plus a term $N \int d\tau \partial_\tau \ln A$ which vanishes owing to periodicity.

We emphasize that during the instanton event, α and $\bar{\alpha}$ are *not* related by complex conjugation. This feature of the instanton solution is familiar, for if one treats the problem of quantum tunneling in a potential $V(x)$ using

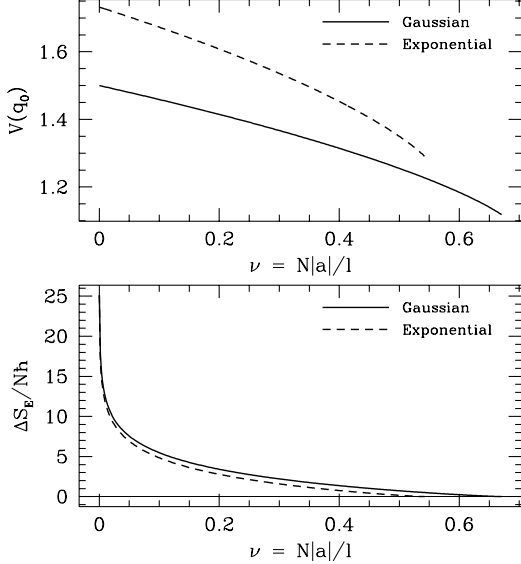


FIG. 3. Numerically obtained results for the energy $V(q_0)$ of the metastable state and action $\Delta S_E/N\hbar$ as a function of ν . Results are shown for the Gaussian and the Exponential trial condensate functions.

coherent states, the saddle point path is determined by the equations

$$\partial z/\partial\tau = -\partial H/\partial\bar{z} \quad (10)$$

$$\partial\bar{z}/\partial\tau = +\partial H/\partial z, \quad (11)$$

where $z = (x + ip)/\sqrt{2}$, $\bar{z} = (x - ip)/\sqrt{2}$, and $H = \frac{1}{2}p^2 + V(x)$. During the instanton event, $\bar{z} \neq z^*$ – indeed $\bar{z} = z^*(-\tau)$ – so the momentum $p(\tau)$ is imaginary.

In fact, we can change variables to (q, p) , where

$$\alpha \equiv \frac{1}{2}(q^2 + iqp^{-1}) \quad (12)$$

$$\bar{\alpha} \equiv \frac{1}{2}(q^2 - iqp^{-1}) \quad (13)$$

so that

$$S_E/\hbar = N \int d\tau \left\{ \frac{3}{4}i(p\dot{q} - q\dot{p}) + \frac{3}{4}(p^2 + q^{-2}) + \frac{3}{4}q^2 - \frac{\nu}{\sqrt{2\pi}}q^{-3} \right\}. \quad (14)$$

Let us define the Hamiltonian

$$H(p, q) = \frac{3}{4}p^2 + \frac{3}{4}q^{-2} + \frac{3}{4}q^2 - \frac{\nu}{\sqrt{2\pi}}q^{-3}. \quad (15)$$

The equations of motion are then

$$-\frac{3}{2}i\dot{q} = \partial H/\partial p \quad (16)$$

$$\frac{3}{2}i\dot{p} = \partial H/\partial q, \quad (17)$$

from which we see that ip is real during the instanton event, as usual.

In figure 2 we show contour plots of $H(p, q)$ and $H(ip, q)$ for $\nu = 0.40$. The minimum of $H(p, q)$ occurs at $(0, q_0)$ while q_1 is the location of the maximum of $V(q)$. The saddle point is traversed during the instanton by p becoming imaginary and ip moving around the contour line $H(ip, q) = V(q_0)$, which encircles the local maximum $(0, q_1)$ of $H(ip, q)$. At $\tau = 0$, ψ describes the nucleated state; this is of course denser, since $q(\tau = 0) = q_n < q_0$.

Since the dynamics preserves $H(ip, q)$, the instanton action is given by

$$S_E/N\hbar = \beta V(q_0) + \frac{3}{2}i \oint_{H(ip,q)=V(q_0)} p dq. \quad (18)$$

The difference $\Delta S_E/N\hbar = S_E/N\hbar - \beta V(q_0)$ is proportional to the area enclosed by the contour.

Integrating out the momentum $p(\tau)$, we obtain the action of equations 3 and 4, with $m^* = \frac{3}{2}$. Stoof [5] states that this is in fact the exact value for Gaussian trial states. Within his approximation scheme, he obtains $m^* \simeq 0.27$.

Similar results are obtained using exponential trial functions [10]

$$\psi(\mathbf{r}, \tau) = A \exp(-\alpha r) \quad (19)$$

$$\bar{\psi} = \bar{A} \exp(-\bar{\alpha} r), \quad (20)$$

from which one derives

$$S_E/\hbar = N \int d\tau \left\{ -\frac{3\dot{\alpha}}{\alpha + \bar{\alpha}} + \frac{1}{2}\alpha\bar{\alpha} + 6(\alpha + \bar{\alpha})^{-2} - \frac{\nu}{32}(\alpha + \bar{\alpha})^3 \right\}. \quad (21)$$

With $\alpha \equiv \frac{1}{2}$ and $\bar{\alpha} \equiv \frac{1}{2}$, one obtains results similar to those for the Gaussian model. Integrating out p again generates equation 3 but with $m^* = 9$ and

$$V(q) = \frac{1}{8}\frac{1}{q^2} + 6q^2 - \frac{\nu}{32}\frac{1}{q^3}. \quad (22)$$

Numerical results (see figure 3) show that for any given value of ν , that the metastable state energy $V(q_0)$ is lower for the Gaussian model. The computed action $\Delta S_E/\hbar$ differs little, however (although the maximum value ν_{\max} is model-dependent).

If q is the condensate radius, the functional form

$$V(q) = bq^{-2} + cq^2 - d\nu q^{-3} \quad (23)$$

is generic. Setting $\partial V/\partial q = 0$ gives $q = q_0$ through

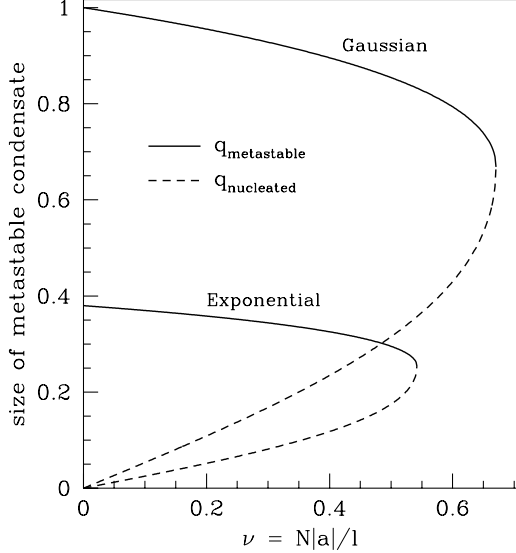


FIG. 4. Trial state results for $q_0(\nu)$ (solid) and $q_n(\nu)$ (dashed).

$$\nu = \frac{2}{3d} q (b - c q^4) \equiv f(q) \quad (24)$$

which is positive for $0 < q < Q \equiv \sqrt[4]{b/c}$. Stable condensates have $q > q_c$ where $f'(q_c) = 0$; this gives $q_c = Q/\sqrt[4]{5} = \sqrt[4]{b/5c}$. Thus ν is restricted to lie in the range $[0, \nu_c]$, where

$$\nu_c = f(q_c) = \frac{8b}{15d} \left(\frac{b}{5c} \right)^{1/4}. \quad (25)$$

Results for the exponential and Gaussian trial condensates are summarized in the following table:

	condensate	b	c	d	m^*
Gaussian	$\psi = A \exp(-\alpha r^2)$	$\frac{3}{4}$	$\frac{3}{4}$	$\frac{1}{\sqrt{2\pi}}$	$\frac{3}{2}$
Exponential	$\psi = A \exp(-\alpha r)$	$\frac{1}{8}$	6	$\frac{1}{32}$	9

The chemical potential is given by

$$\mu = -\frac{1}{3} b q_0^{-2} + \frac{7}{3} c q_0^2, \quad (26)$$

hence we find

$$\nu = 0: q = \sqrt[4]{b/c}, \mu = 2\sqrt{bc} \quad (27)$$

$$\nu = \nu_c: q = \sqrt[4]{b/5c}, \mu = \mu_c \equiv \frac{2}{3\sqrt{5}} \sqrt{bc}. \quad (28)$$

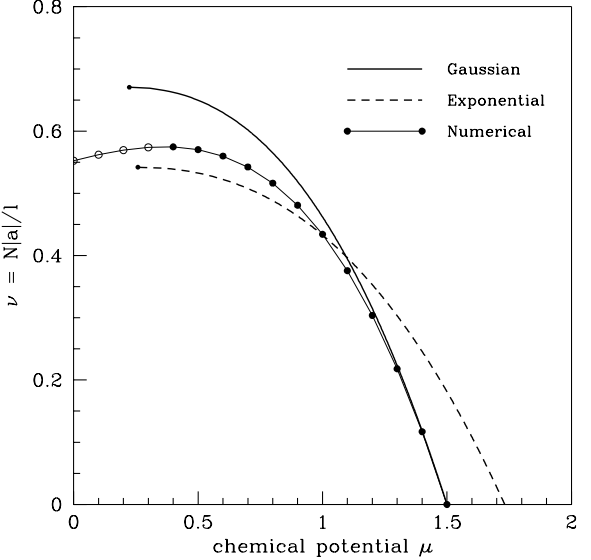


FIG. 5. Scaled particle number *versus* chemical potential for both Gaussian and exponential models. For $\mu < \mu_c$, the condensate is unstable; the curves terminate in a dot at these points. The numerical results obtained by solving the Bogoliubov equations are shown for comparison. Open circles denote unstable condensates.

Thus, in the vicinity of the critical point $q = q_c$, one has

$$\frac{\nu}{\nu_c} = 1 - \frac{5}{288} \left(\frac{\mu}{\mu_c} - 1 \right)^2 + \dots \quad (29)$$

III. BEYOND THE COLLECTIVE COORDINATE APPROACH

We now discuss a full solution of the GP equations, where all degrees of the condensate are retained. We begin with the condensate itself and the real time Bogoliubov equations for excited states. We begin with the nonlinear Schrödinger equation for $\phi \equiv \sqrt{|g|} \psi$,

$$i\partial_t \phi = -\frac{1}{2} \nabla^2 \phi + \frac{1}{2} r^2 \phi - (\bar{\phi} \phi) \phi - \mu \phi, \quad (30)$$

where μ is the dimensionless chemical potential in units of $\hbar\omega$ (we now work in the grand canonical ensemble). We are interested in stationary states, and we consider only real, radially symmetric solutions, for which we write $\phi(r) = R(r)/r$. The radial wave equation for $R(r)$ is

$$-\frac{1}{2} \frac{d^2 R}{dr^2} + \left(\frac{1}{2} r^2 - \mu \right) R - \frac{R^3}{r^2} = 0 \quad (31)$$

subject to the boundary conditions $R(0) = R(\infty) = 0$. We solved this equation on a one-dimensional grid and

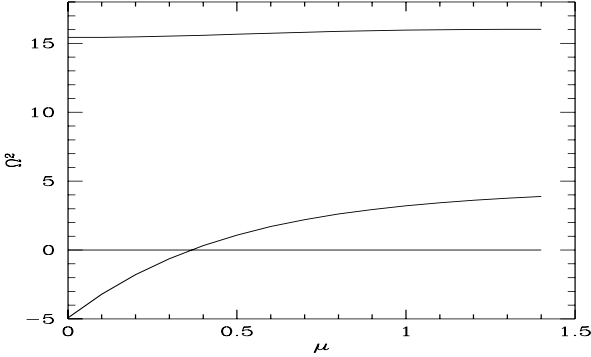


FIG. 6. The three lowest values of Ω^2 , eigenfrequencies of the Bogoliubov equations, as a function of the chemical potential. A negative Ω^2 indicates an unstable condensate.

used a relaxation method [11]. The size of the system was chosen large enough to capture the structure of the wave function. We used as many as 1,000 grid points in the range $r \in [0, 10]$. The results were checked for independence on the system size. This was done for various positive values of the chemical potential μ ; we obtained the ground and several excited states. The number of atoms is given by $N = 4\pi\nu/|g|$, with

$$\nu = \int_0^\infty dr R^2(r) . \quad (32)$$

The dependence of ν on the chemical potential is shown in figure 5 along with the predictions of the trial condensate models. Stationary condensates exist for all values of $\mu < 1.5$. The stability of these states can only be checked by a numerical integration of the time dependent nonlinear Schrödinger equation (NLSE) [1], or, as we did, by computing the spectrum of fluctuations above these condensates.

Once the ground state solution R_0 is found, we solve for the spectrum of fluctuations, writing $\phi = \phi_0 + \eta$, with $\phi_0 = R_0(r)/r$. This leads to the Bogoliubov equations [12,13]

$$\begin{aligned} \Omega u &= \left(-\frac{1}{2}\nabla^2 + \frac{1}{2}r^2 - \mu - 2|\phi_0|^2 \right) u - \phi_0^2(r) v \\ -\Omega v &= \left(-\frac{1}{2}\nabla^2 + \frac{1}{2}r^2 - \mu - 2|\phi_0|^2 \right) v - \phi_0^{*2}(r) u \end{aligned} \quad (33)$$

where

$$\eta(\mathbf{r}, t) = u(\mathbf{r}) \exp(-i\Omega t) + v^*(\mathbf{r}) \exp(i\Omega^* t) . \quad (34)$$

The condensate function ϕ_0 is taken to be real. Note that $(u, v) = (\phi_0, -\phi_0)$ is a zero mode.

Taking advantage of the radial symmetry of ϕ_0 , one can classify the excited states by angular momentum and

compute the excitation energies; the spectrum was investigated in [12]. In figure 6 we plot the three lowest values of Ω^2 versus μ . Consistent with previous work [12], we find that for $\mu < 0.4$ there is a purely imaginary eigenfrequency reflecting the instability of the stationary state. The inverse of the imaginary part of Ω gives the typical time for the instability to grow. For larger values of the chemical potential (lower values of N) the unstable mode crosses the zero mode and the spectrum becomes that of a stable condensate, as in the repulsive case. We find the stability boundary lies at $\nu = 0.57$, in agreement with the results of ref. [1].

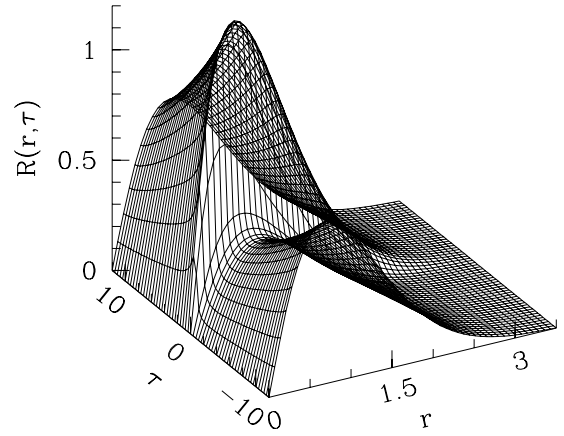


FIG. 7. Plot of the radial wave function of the bounce for $\mu = 0.7$. The system size was $\tau \in [-12, 12]$ and $r \in [0, 3.5]$. The parameter δ (see equation 42) is 0.028.

We now compute the tunneling rate using the familiar instanton formalism [7]. In order to compute the instanton action, we must solve the following equations of motion derived from equation 2. Adding a chemical potential term, we obtain the equations

$$-\partial_\tau \phi = -\frac{1}{2}\nabla^2 \phi + \left(\frac{1}{2}r^2 - \mu \right) \phi - (\bar{\phi}\phi)\phi \quad (35)$$

$$+\partial_\tau \bar{\phi} = -\frac{1}{2}\nabla^2 \bar{\phi} + \left(\frac{1}{2}r^2 - \mu \right) \bar{\phi} - (\bar{\phi}\phi)\bar{\phi} \quad (36)$$

subject to periodic boundary conditions on the interval $\tau \in [-\frac{1}{2}\beta, \frac{1}{2}\beta]$, where β is the inverse temperature (we are interested in the $\beta \rightarrow \infty$ limit). Note that these equations yield the imaginary time version of the continuity equation,

$$i\partial_\tau \rho + \nabla \cdot \mathbf{j} = 0 , \quad (37)$$

with

$$\rho = \bar{\phi}\phi , \quad \mathbf{j} = \frac{1}{2i}(\bar{\phi}\nabla\phi - \phi\nabla\bar{\phi}) . \quad (38)$$

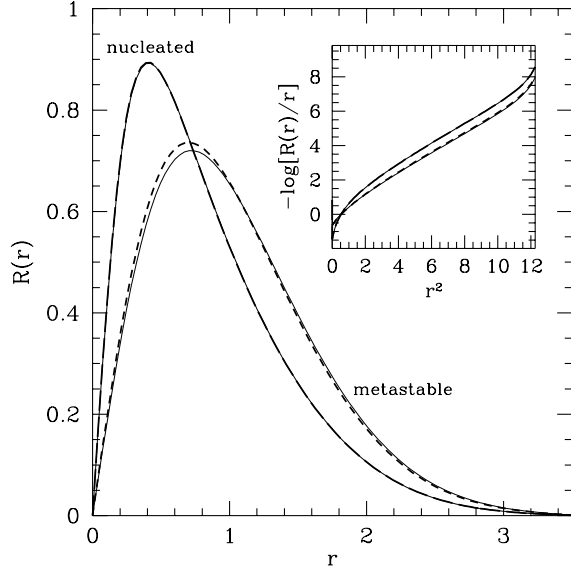


FIG. 8. The metastable state and the nucleated state for the bounce of figure 7. The inset shows $-\ln \phi$ vs. r^2 ; deviations from pure Gaussian behavior are apparent. Thin solid lines show the corresponding results for periodic solutions.

Thus, the total particle number $N = \int d^3r \rho(\mathbf{r})$ is conserved by the evolution equations, since \mathbf{j} vanishes as $r \rightarrow \infty$. It should be emphasized that equations 35 and 36 are *not* complex conjugate pairs. However, the instanton solutions of interest all have the symmetry

$$\bar{\phi} = \phi^*(\mathbf{r}, -\tau), \quad (39)$$

where $(*)$ denotes complex conjugation [14]. Substituting this into equation 35 leads to a nonlocal equation in (imaginary) time for ϕ . Nevertheless, a straightforward application of Newton's method may be used to obtain a numerical solution [9]. The equations admit a static solution, $\phi(\mathbf{r}, \tau) = \phi_0(r)$, describing the metastable state. In the limit $\beta \rightarrow \infty$, the nontrivial bounce solution satisfies $\phi_b(\mathbf{r}, \tau) = \phi_0(r)$ at $\tau = \pm \frac{1}{2}\beta$, while describing a denser nucleated condensate at $\tau = 0$. The tunneling rate, obtained by summing over all multibounce solutions [7], is

$$\Gamma = A \exp(-\Delta S_E/\hbar) \quad (40)$$

where $A = \det^{-1/2}[\delta^2 S_E]$ is the fluctuation determinant prefactor, and ΔS_E is the difference between the Euclidean actions of the bounce and static solutions to (35,36). Since the energy is preserved by the dynamics, we obtain

$$\frac{\Delta S_E}{N\hbar} = \frac{\int d\tau \int d^3r \bar{\phi}_b \partial_\tau \phi_b}{\int d^3r \bar{\phi}_b \phi_b}. \quad (41)$$

The numerical method used to solve for $\phi_b(\mathbf{r}, \tau)$ is described in ref. [9]. Briefly, we look for real, radially sym-

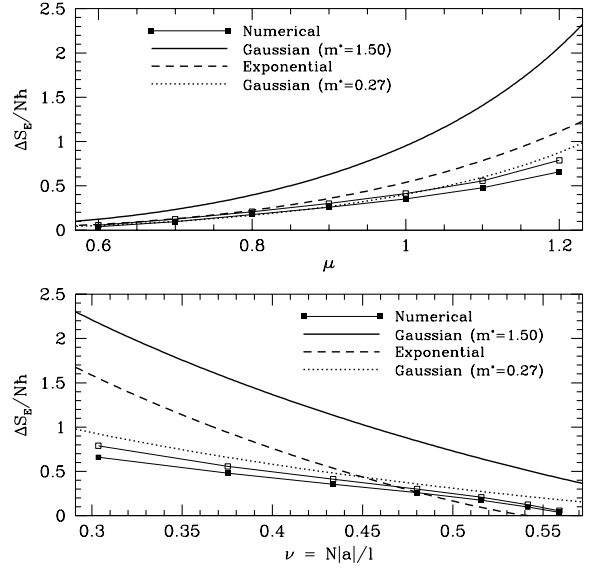


FIG. 9. A comparison of the numerically obtained instanton action with various trial state predictions of $\Delta S_E/\hbar$. Filled squares represent numerical data with aperiodic boundary conditions; open squares denote periodic boundary conditions.

metric solutions, $\phi_b(r) = R_b(r)/r$. We discretize space-time and write (35,36) as a set of nonlinear equations which we solve using the Newton-Powell method [17]. This process demands an initial guess for the bounce solution, which we took to be an interpolation between the static $\phi_0(r)$ at $\tau = -\frac{1}{2}\beta$ and a somewhat denser Gaussian profile at $\tau = 0$. It is necessary to choose this guess to be asymmetric in imaginary time about $\tau = 0$.

When β is finite, periodic solutions will deviate from the static ϕ_0 at $\tau = \pm \frac{1}{2}\beta$. We enforced $\phi(r, -\frac{1}{2}\beta) = \phi_0(r)$ which results in non-periodicity of the bounce solution. We confirm that as we increase β that $\phi(r, +\frac{1}{2}\beta)$ approaches $\phi_0(r)$ while the central structure around $\tau \approx 0$ does not change appreciably. It is the central part of the bounce which contributes most to (41). A measure of the aperiodicity is

$$\delta = \frac{\int_0^\infty dr |R_b(r, -\frac{1}{2}\beta) - R_b(r, +\frac{1}{2}\beta)|}{\int_0^\infty dr R_b(r, -\frac{1}{2}\beta)}. \quad (42)$$

We increased β until $\delta < 0.05$, at which point we deemed our solution a good approximation of the $\beta = \infty$ bounce. The radial coordinate was chosen to extend from $r = 0$ to a maximum $r = L$, where L was chosen to accommodate the metastable state. We required $R_b(L, \tau) < 0.01$ in all cases, where typically we took $L = 5$.

Another approach is to require periodicity for all β , as is necessary when computing the finite temperature

instanton solution. In this case, the wavefunctions at $\tau = \pm\frac{1}{2}\beta$ agree with each other, but not with the metastable solution of the NLSE. Of course agreement is recovered in the $\beta \rightarrow \infty$ limit. In figures 8 and 9 we compare the results of these two approaches for $\beta = 24$. We found the aperiodic solution systematically yielded a lower value of $\Delta S_E/N\hbar$. The agreement between the two schemes for $\beta = 24$ is at the 30% level, with better agreement for larger values of μ .

In figure 7 we plotted the radial wave function of the bounce, $R_b = r\phi_b$, for $\mu = 0.7$. We stress that ϕ_b is interpretable as a condensate wavefunction only at $\tau = \pm\frac{1}{2}\beta$ and at $\tau = 0$, where it represents the metastable and nucleated condensates, respectively. In figure 8 we plot, also for $\mu = 0.7$, the radial wavefunctions $R_0(r, -\frac{1}{2}\beta)$ and $R_b(r, 0)$ corresponding to the metastable and nucleated states, respectively. Real time evolution of the nucleated state using the nonlinear Schrödinger equation describes an ever collapsing condensate. This is analogous to a tunneling particle rolling down the hill after it emerges from the tunnel barrier. In figure 10 we show the radial condensate density, $r^2 |\phi(r)|^2$, developing towards collapse as the nucleated state evolves in real time according to the NLSE [15].

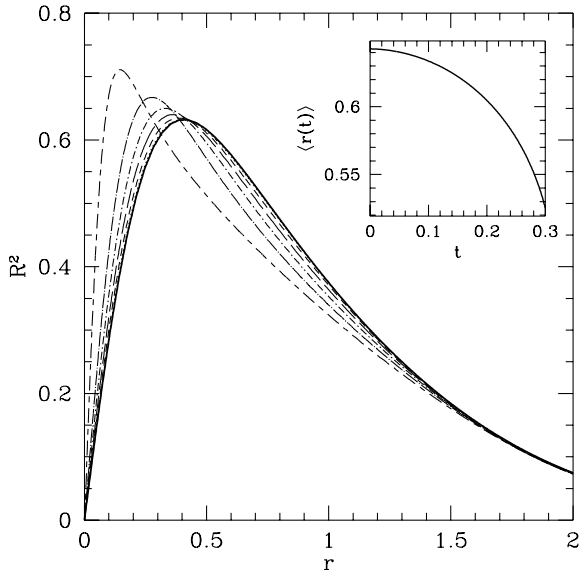


FIG. 10. Real time evolution of the nucleated condensate (dark solid curve) for $t = 0.05$, $t = 0.10$, $t = 0.15$, $t = 0.20$, $t = 0.25$, and $t = 0.30$. N is accurately conserved by the integration. The inset shows the collapse of the condensate as measured by $\langle r(t) \rangle$.

We worked in the range $0.6 \leq \mu \leq 1.2$. We could not reach larger values of μ because these demanded a very large β which increased the calculation time [16]. For the smaller values of μ the bounce becomes flatter and loses its temporal structure. Eventually $\Delta S_E/N\hbar \rightarrow 0$ as μ decreases to its minimum allowed value of $\mu_{\min} \simeq 0.4$. In

this region, we only obtained convergence to the trivial (metastable) solution.

A comparison of our numerical results with those of the various collective coordinate theories is shown in figure 9. Apparently Stoof's approximation $m^* = 0.27$ is in much better agreement with the data than $m^* = \frac{3}{2}$ derived from the Gaussian trial states of equations (6, 7). No other parameters have been adjusted.

IV. CONCLUSIONS

In this paper, we investigated the decay of metastable Bose-Einstein condensates with attractive interactions confined in a parabolic trap. The decay rate was calculated using the instanton formalism, applied to the Gross-Pitaevskii action, $S_E[\psi, \bar{\psi}]$. The field theory can be reduced to an effective quantum mechanics problem by focusing on a collective coordinate which describes the width of the condensate, as was first done by Stoof [5]. We went beyond the collective coordinate approach, numerically solving for the instanton field configuration $\psi(\mathbf{r}, \tau)$. This was accomplished by rendering the nonlinear partial differential equations for ψ and $\bar{\psi}$ as a large set of nonlinear equations on a space-time lattice and solving them via the Newton-Powell method. We can thereby derive the nucleated state wavefunction, which describes the condensate at the instant it emerges from the tunneling barrier. The nucleated state, evolved according to the real time nonlinear Schrödinger equation, collapses to an arbitrarily dense state for which the attractive GP model is no longer a good approximation. While the numerically obtained metastable and nucleated states show deviations from pure Gaussian behavior, a comparison of the leading contribution to the semiclassical tunneling rate reveals moderate agreement between numerical values and those obtained from Gaussian approximations to the (dynamical) condensate wavefunction. Adjusting only the collective coordinate effective mass m^* puts the two schemes in quite good agreement. Thus we conclude that the collective coordinate description adequately captures the essential physics of the tunneling process.

V. ACKNOWLEDGEMENTS

This work is in large part a continuation of work performed with H. Levine, to whom we are grateful for numerous discussions and suggestions. We also thank D. S. Rokhsar and H. T. C. Stoof for discussions. JAF acknowledges support from the Brazilian Agency CNPq.

VI. BIBLIOGRAPHY

- [1] P. A. Ruprecht *et al.*, *Phys. Rev. A* **51**, 4704 (1995).
- [2] E. R. I. Abraham *et al.*, *Phys. Rev. Lett.* **74**, 1315 (1995).
- [3] Of course, at atomic length scales the hard sphere nature of the atoms is manifest and the potential is repulsive.
- [4] C. C. Bradley, C. A. Sackett, and R. G. Hulet, *Phys. Rev. Lett.* **78**, 985 (1997).
- [5] H. T. C. Stoof, *J. Stat. Phys.* **87**, 1353 (1997). See also M. Ueda and A. J. Leggett, preprint [cond-mat/9801196](#).
- [6] L. P. Pitaevskii, *Sov. Phys. JETP* **13**, 451 (1961); E. P. Gross, *J. Math. Phys.* **4**, 195 (1963).
- [7] S. Coleman, The Uses of Instantons in *Aspects of Symmetry* (Cambridge University Press, New York, 1985); M. Stone, *Phys. Lett.* **67B**, 186 (1977).
- [8] J. W. Negele and H. Orland, *Quantum Many-Particle Systems* (Addison-Wesley, Palo Alto, California, 1988).
- [9] J. A. Freire, D. P. Arovas, and H. Levine, *Phys. Rev. Lett.* **79**, 5054 (1997).
- [10] As $r \rightarrow 0$ there can be no linear term in $\psi(r)$, so exponential behavior is wrong in the vicinity of the origin.
- [11] W. H. Press, S.A. Teukolsky, W. T. Vetterling and B. P. Flannery, *Numerical Recipes* (Cambridge University Press, Cambridge, 1986).
- [12] K. G. Singh and D. S. Rokhsar, *Phys. Rev. Lett.* **77**, 1667 (1996); M. Edwards, P.A. Ruprecht, K. Burnett, R.J. Dodd, and C.W. Clark, *Phys. Rev. Lett.* **77**, 1671 (1996).
- [13] A. L. Fetter, *Phys. Rev. A* **53**, 4245 (1996); F. Dalfovo, S. Giorgini, M. Giulleumas, L. Pitaevskii, and S. Stringari, *Phys. Rev. A* **56**, 3840 (1997).
- [14] Because the metastable state was real we looked only for real solutions.
- [15] The integration of the time dependent NLSE, equation 30, was done using a split-step method. The Laplacian part is integrated using a Crank-Nicholson method and the local part in integrated exactly. This results in scheme accurate to $\mathcal{O}(\Delta t)$.
- [16] The largest grid used had 30,000 points, 100 in the radial direction and 300 in the time direction. All calculations were performed in a PC running a Pentium 133MHz processor.
- [17] M. J. D. Powell, in *Numerical Methods for Nonlinear Algebraic Equations*, P. Rabinowitz ed. (Gordon and Breach, London, 1970).